Vol. 495: 27–38, 2014
doi: 10.3354/meps10582

MARINE ECOLOGY PROGRESS SERIES
Mar Ecol Prog Ser

Published January 9

Environmental interference factors affecting detection range in acoustic telemetry studies using fixed receiver arrays

Noelle H. Mathies[1,*], Matthew B. Ogburn[2], Greg McFall[3], Sarah Fangman[3]

[1]Savannah State University Marine Sciences Program, 3219 College Street, Savannah, Georgia 31404, USA
[2]Smithsonian Environmental Research Center, 647 Contees Wharf Road, Edgewater, Maryland 21037, USA
[3]Gray's Reef National Marine Sanctuary, 10 Ocean Science Circle, Savannah, Georgia 31411, USA

ABSTRACT: Historically, acoustic telemetry studies tracking movement of aquatic organisms have lacked rigorous, long-term evaluations of detection range. The purpose of the present study was to identify potential sources of variability in long-term acoustic telemetry data, focusing specifically on environmental variability. The study was conducted for 15 mo in Gray's Reef National Marine Sanctuary, Georgia, USA, using 2 submersible Vemco VR2W hydrophone receivers and 2 stationary range test transmitters (controls). Tag detections (±1 SE) decreased from 54.2 ± 2.5 to 11.4 ± 0.5 detections d^{-1} as transmission distance increased from 100 to 300 m. Detections varied seasonally (likely due to stratification), with the direction of flood and ebb tidal currents (12.4 h cycle), and with tidal current speed (6.2 h cycle). Tides explained up to 92% of the short-term variability in hourly detection data. Detections also increased or decreased during episodic weather events depending on the season and type of event. These results suggest that stationary control tags are useful for characterizing variability in sound transmission in open water marine acoustic telemetry studies.

KEY WORDS: Long-term monitoring · Seasonal variation · Signal-to-noise · Time series analysis · Tides · Stratification

INTRODUCTION

Understanding daily movement patterns and documenting long-distance migrations are critical components of the conservation and management of marine fisheries, especially when marine protected areas are employed as a management tool. The rapid expansion of the use of acoustic telemetry has advanced the study of movement and migration of flounder *Pseudopleuronectes americanus*, cuttlefish *Sepia apama*, tiger sharks *Galeocerdo cuvier*, and many other organisms (DeCelles & Cadrin 2010, Heithaus et al. 2010, Payne et al. 2010), but its limitations have received little attention in the literature. Acoustic telemetry uses sound waves to transmit and record the presence of an organism fitted with an acoustic tag. Time since deployment is thought to affect receiver performance due to battery life, memory capacity, or biofouling (Heupel et al. 2008). However, environmental conditions also affect the detectable range of acoustic signals (Heupel et al. 2006, Simpfendorfer et al. 2008). A wide range of environmental (including natural physical structures, water column properties, bubbles, and biological noise) and anthropogenic factors (including boat motors, other mechanical noise, and deployment of multiple acoustic tags) can interfere with signal transmission and cause patterns in detections that could be misinterpreted as movement of tagged individuals (Heupel et al. 2006, Kuperman & Roux 2007, Simpfendorfer et al. 2008, Payne et al. 2010, Topping & Szedlmayer 2011). Unfortunately, the effects of environmental variability on acoustic telemetry remain largely unstudied.

*Corresponding author: noelle.hawthorne@gmail.com

Placing stationary tags (controls) in the study environment and monitoring their detection efficiency over time can aid in determining the various effects of environmental variability on sound transmission. For example, acoustic detections of 7 tagged Australian giant cuttlefish *Sepia apama* and 3 stationary control tags were higher at night than during the day (Payne et al. 2010). After correcting for the diel environmental variability using control tag data, a reverse behavioral pattern was observed in which cuttlefish were more likely to be detected during the day than during the night. Increased signal collisions due to nighttime biological noise from snapping shrimp (Alpheidae) was the proposed mechanism for decreased nightly detections, but this hypothesis was not formally investigated (Payne et al. 2010). Temperature, time of day, lunar cycle, and especially water movement have also been observed to affect tag detections in ocean environments off the western coast of Australia, but a formal investigation of mechanisms was not completed (How & de Lestang 2012).

While it is likely that a variety of environmental factors might affect acoustic telemetry, the scientific literature lacks a comprehensive study of the multiple environmental drivers that can potentially interfere with signal transmission in studies of both long and short durations. The purposes of our long-term study were to identify the specific environmental factors interfering with acoustic transmission and determine the extent to which they affect detection efficiency. In the study, detection efficiency was defined as the number of actual detections divided by the number of expected detections. Detections were compared with 3 types of environmental factors (1) seasonal cycles, (2) short-term (tidal and diel) cycles, and (3) event-driven variability (e.g. weather, time since deployment, biofouling).

MATERIALS AND METHODS

Study site

The present study was conducted in Gray's Reef National Marine Sanctuary, a protected area managed by the US National Oceanic and Atmospheric Administration (NOAA), located about 40 nautical miles southeast of Savannah, Georgia (USA). The sanctuary spans 57 km^2 and contains 4 different habitat classifications, including sparsely colonized hard bottom, densely colonized hard bottom, rippled sand, and flat sand (Kendall et al. 2005). The substratum of the sanctuary is calcitic and aragonitic sandstone, on which large invertebrates attach and form the basis of the reef community. Seventy-five percent of the sanctuary seafloor is composed of flat and rippled sand, and densely colonized cemented sandstone ledges make up <1% of its total area (Kendall et al. 2005). The average depth is 18 m and ledges typically have a vertical relief of 0.5 m (Kendall et al. 2005).

Control tag and receiver deployment design

Two submersible Vemco LTD VR2W hydrophone receivers and 2 V13 range test transmitters (control tags) were deployed within Gray's Reef from 1 February 2011 to 15 May 2012 (Fig. 1). Receivers were placed where fishing success was greatest in a fish tagging project that started in 2008. Receiver detection ranges were tested during the initial deployment in March 2008 using range test tags, and the 50% reliable detection range was determined to be 200 m (Carroll 2010). The placement of control tags was determined by both the relative absence of tagged fish, which limited tag interference and prevented the overloading of receiver memory capacity, and by distances to the receivers, which were chosen to evaluate the validity of the 200 m detection range over time. Control1 was located 103 m from ReceiverC and about 282 m from ReceiverD (Fig. 1). Control2 was located 220 m from ReceiverC and 167 m from ReceiverD (Fig. 1). The tags were set to send a signal every 8 min at a frequency of 69 kHz. At a much higher ping rate of random intervals from 60 to 180 s, receivers had sufficient data storage capacity for a minimum deployment of 208 d and likely greater than 300 d (Heupel et al. 2006). Therefore, with 2 control tags with a much lower ping rate and few fish frequenting the 2 receivers, no special download measures were taken for the control and receiver array that were not already in place for fish receivers in the rest of the sanctuary.

Receivers and control tags were suspended 1.5 m above the bottom (14 to 18 m) using anchored buoy lines. The specific configuration reduced the amount of noise interference from surface waves and vessel traffic (Heupel et al. 2006). An anchoring system held the buoy lines, which consisted of a 10 cm diameter stainless steel rod that weighed from 45 to 70 kg and measured 90 to 120 cm in length. Two stainless steel legs were welded to the stainless steel anchor to prevent rolling. Each 240 cm buoy line consisted of a 1 cm diameter line from the base of the buoy to the top of the anchor. The buoy line was held in the water column using two 20 cm diameter subsurface buoys

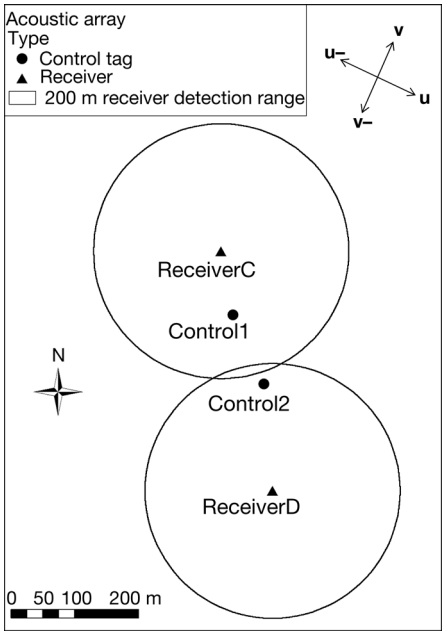

Fig. 1. Orientation of Vemco VR2W acoustic receivers (black triangles) and stationary V13 control tags (black circles). Large open circles represent the determined reliable 200 m 50% detection range (Carroll 2010). The cross-shelf (**u**) and along-shelf (**v**) arrows represent the orientation of positive and negative wind and current vectors (note that **u** and **v** refer to the direction the wind is from and that current flows toward). Latitude and longitude are not shown so that the location of the acoustic array within the sanctuary remains confidential

with a lift capability of 2.46 kg. The buoys were enclosed in nylon stockings to reduce the amount of fouling growth, to facilitate cleaning of growth that did occur, and to reduce potential loss of buoyancy.

Receivers had an internal clock set to UTC, which was checked for accuracy when initialized and recording was started. The receivers were wrapped in electrical tape and then placed inside a nylon stocking when deployed to reduce fouling growth, which could potentially affect signal reception. SCUBA divers secured the receivers and control tags to the buoy line with plastic cable ties. Divers performed maintenance on each receiver and control tag set-up every 2 to 6 mo. Buoys were checked for adequate buoyancy, and buoy lines were examined for strength. Clean, replacement receivers were re-initialized before deployment during each maintenance event to limit any potential drift clock error that may have occurred. Existing receivers were exchanged for a clean receiver with empty memory on each dive. The data were downloaded and stored onto a laptop computer. Control tags were cleaned and scraped of fowling growth as much as possible.

Environmental data

Environmental data were collected from NOAA's National Data Buoy Center (NDBC) weather buoy 41008 deployed within the sanctuary. The buoy, located about 3.5 km north of Control1 (Fig. 1), recorded water temperature, wind speed and direction, current speed and direction, and wave data (Fig. 2). The cross-shelf (**u**) and along-shelf (**v**) vectors represent the orientation of positive and negative wind and current vectors (note that **u** and **v** refer to the direction the wind is from and that current flows toward). Before analysis, wind data were converted into cross-shelf (**u**; positive from 120°) and along-shelf (**v**; positive from 30°) wind stress vectors following Large & Pond (1981) and using the meteorological convention for the direction the wind was coming from. Raw wave energy data were converted to swell energy to reflect the power of longer wavelengths (0.04 to 0.10) that have the potential to affect turbidity at the bottom. Data from the 600 kHz RD Instruments Workhorse acoustic Doppler current profiler (ADCP) were used to generate current profiles. The ADCP recorded the current direction and speed at 1 m intervals from 2 to 18 m depth (binned hourly current vector data downloaded from NDBC). Current recordings at 13 m were used for our study because they were the most reliable recordings taken (based on ADCP data quality records) closest to the depth of the receivers and control tags. The cross-shelf (**u**; positive 120°) and along-shelf (**v**; positive from 30°) current vectors were calculated following the oceanographic convention of the direction the current was flowing towards (Fig. 1). These axes were chosen from visual inspection of the current data so that **u** represented the primary axis of flood and ebb tidal currents and **v** represented currents that were perpendicular to the dominant tidal currents. The cross-shelf and along-shelf components of the current vectors were calculated at hourly intervals. ADCP data were not available after February 2012 due to equipment failure.

Indices of stratification were calculated by comparing subtidal, diurnal band currents among depths. Throughout the rest of our paper, stratification is defined by 2 indices calculated based on depth-varying currents within the sanctuary. Synergism between the sea breeze and the Coriolis force drive diurnal band currents at Gray's Reef with a 3-layer flow pattern under stratified conditions and a 2-layer pattern under unstratified conditions (Edwards & Seim 2008). Thus differences in diurnal band currents among depths can be used as a proxy for strati-

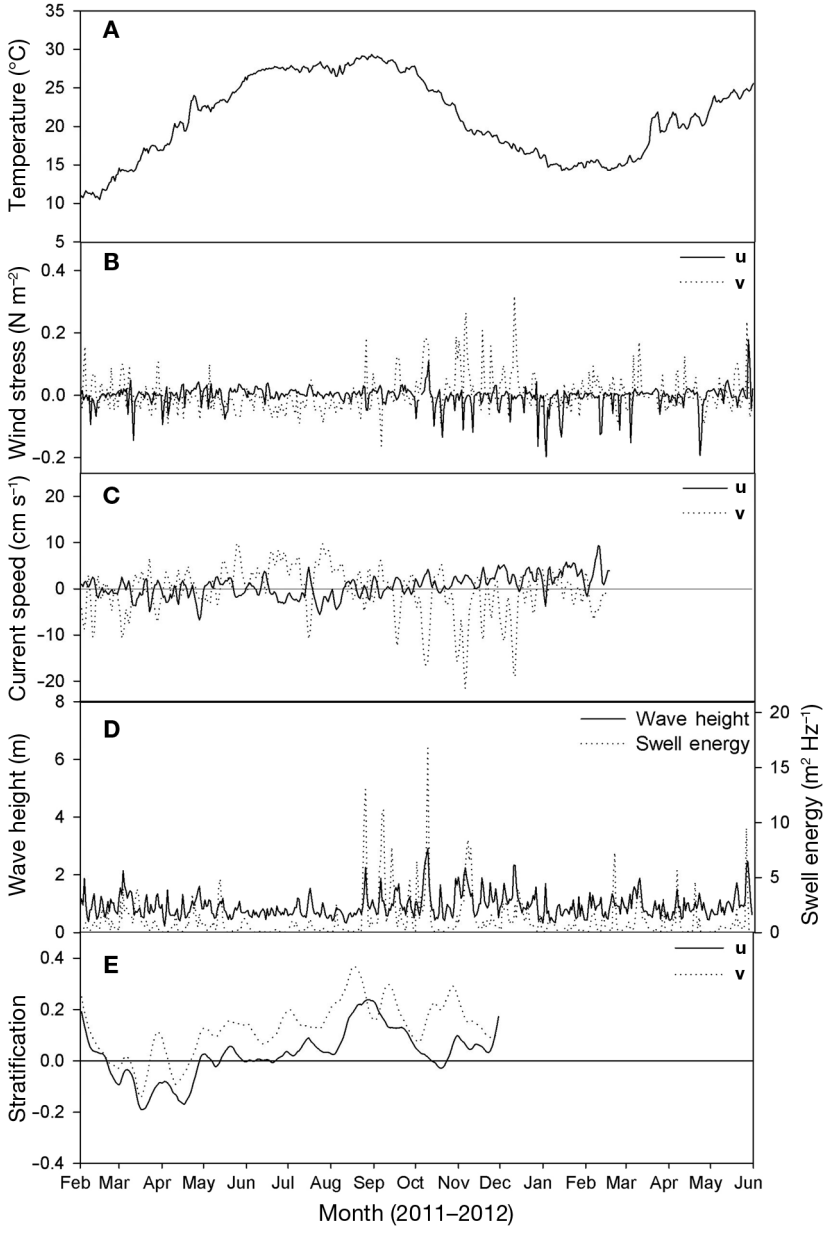

Fig. 2. Daily environmental data recorded at Gray's Reef National Marine Sanctuary. Environmental data include: (A) temperature, (B) cross-shelf (**u**) and along-shelf (**v**) wind stress vectors, (C) cross-shelf (**u**) and along-shelf (**v**) current vectors smoothed with a 71 h moving average, (D) wave height and swell energy, and (E) stratification indices calculated from **u** and **v** current vectors. Swell energy was calculated as the sum of the wave energy of the longer wave frequencies of 0.04 to 0.10 waves s^{-1}. Stratification indices are the difference in subtidal, diurnal band currents between 8 and 13 m. Current vector data (and stratification indices derived from them) were not available after February 2012 due to equipment failure

fication. The general approach was to remove all semidiurnal and long-term variability from the raw current data and compare currents among depths, based on the methods of Edwards & Seim (2008). ADCP data from 2 to 13 m depth were analyzed using empirical orthogonal functions (EOFs) and the first EOF, composed primarily of tides, was subtracted from the raw data at each depth. The new, non-tidal current data were filtered using a bandpass filter to remove short- (<15 h) and long-term (>28 h) variability, leaving residuals that were composed only of the diurnal band currents. Current residuals from 8 m depth were subtracted from those from 13 m depth to generate an index of stratification based on the changes in current direction with depth. This process was conducted on current data for both the cross-shelf and along-shelf currents, resulting in 2 rough indices of stratification (Fig. 2) from the best available data.

Statistical analyses

Statistical analyses were designed to address 3 types of variability that were evident from visual inspection of the detection data: long-term (seasonal) cycles, short-term (<48 h) cycles, and episodic events (weather, receiver exchange, tag maintenance). A previous study did not find variability around the spring and neap tidal cycle or lunar cycle in fish detection records at Gray's Reef (Carroll 2010) nor were there obvious patterns related to these cycles in the control tag data.

Correlation analysis was used to compare the total number of control tag detections each day to seasonally varying environmental data using MATLAB© (MathWorks). Both daily control tag detections for each tag and receiver pair and daily environmental data (temperature, swell energy, wave height, cross- and along-shelf wind stress, cross- and along-shelf current, and the cross- and along-shelf stratification indices) were processed before analysis, with a low-pass filter to remove short-term variability (<10 d). Correlations were considered significant if they exceeded the 95% confidence interval calculated following Wing et al. (1995).

Short-term cycles were analyzed using wavelet analysis and compared with environmental variables using cross-Fourier analysis. The wavelet analysis (conducted in MATLAB) followed the methods of Torrence & Compo (1998) and was used to identify cycles in hourly detection data, determine the period lengths of dominant cycles, and determine whether the dominant period length changed over the duration of the study. Statistical significance of peaks in the global wavelet spectrum was determined using a 95% confidence interval (Torrence & Compo 1998). If no peaks in the global wavelet spectrum were significant for the entire time series, the most variable portion of the data was extracted and reanalyzed. This was done for Control1/ReceiverC (13 April to 1 June 2011) and Control2/ReceiverD (14 April to 26 July 2011). The tag and receiver pair nomenclature Control1/ReceiverC represents transmissions from tag Control1 detected on the hydrophone of ReceiverC.

Cross-Fourier analysis allowed for direct comparisons of tag detections and environmental data at the significant period lengths identified using the wavelet analysis. These analyses (also conducted in MATLAB) compared hourly detection data with hourly environmental data including cross-shelf tidal current speed (the absolute value of the current vector **u**; 6.2 h cycle length; 3.87 cycles per day [cpd]), tidal current direction (the current vector **u**; 12.4 h; 1.94 cpd), and the diel cycle (24.0 h; 1.00 cpd). It should be noted that the cross-Fourier analysis was calculated based on frequency intervals that, when converted to units of period length, have smaller intervals at the lower end of the scale and larger intervals at the upper end of the scale. The consequence of this is that when evaluating diel (24.0 h) variability, the closest period length tested is 25.6 h for cross-Fourier analyses. The same is true in this analysis for evaluating tidal current direction (12.6 h) variability; the closest period length tested was 12.8 h. The diel cycle was simulated using values of 0 for day and 1 for night. The result of the cross-Fourier analysis, the cross power spectral density (CPSD), was used to identify cycles that were common between environmental and detection datasets. The strength of covariance between detections and environmental data was evaluated by calculating the squared-coherence at the cycle lengths of peaks in the CPSD. Squared-coherence provides an estimate of the percent variability in tag detections that could be explained by the environmental variable, as in Shanks (2006).

Short-term episodic events were analyzed by comparing detections before and after tag and receiver maintenance events, as well as before and during storm events, using the Wilcoxon signed rank test. For maintenance events, the sums of detections occurring 24.0 h before and 24.0 h after maintenance were compared to examine the effect of the removal of biofouling organisms and receiver replacement. Storm events were defined as peaks or valleys in the daily along-shelf (**v**) wind stress data that exceeded the average of the absolute value of **v** by more than 1 standard deviation. Winter storms (n = 15) and summer storms (n = 6) were analyzed separately. The sum of daily detections for all 4 tag and receiver pairs was compiled for 1 d before and 1 d during the peak along-shelf wind, which is the dominant axis for increased winds during storms on the Georgia coast.

RESULTS

There was significant variability in detections with respect to distance between tags and receivers. From 1 February 2011 to 16 May 2012, Control1 was detected a total of 25 544 times (54.2 ± 2.5 detections d^{-1}; all means are presented as ±1 SE) on ReceiverC at a distance of 103 m (Fig. 3A). The same tag was detected only 5356 times (11.4 ± 0.5 detections d^{-1}) on ReceiverD at a distance of 282 m (Fig. 3B). Control2 logged 14 826 detections (31.5 ± 1.5 detections d^{-1}) on ReceiverC, 220 m away, and 27 474 detections (58.3 ± 2.7 detections d^{-1}) on ReceiverD, a distance of only 167 m (Fig. 3). All 4 tag and receiver pairs had a minimum of 0 detections d^{-1} and a maximum of 172 to 180 detections d^{-1} for the duration of the study (Fig. 3). With a maximum of 180 detections d^{-1}, the best tag and receiver pair (Control2/ReceiverD) averaged only 36.2% of possible transmissions for the duration of the study at a distance of 167 m, a shorter distance than the previously estimated 50% detection range of 200 m.

Seasonal variability

There was a distinct seasonal pattern, with high detections in winter and low detections in summer. Seasonally varying environmental data, including temperature, swell energy, along-shelf (**v**) currents, and the along-shelf stratification index were all significantly correlated with daily detection data from all 4 tag and receiver pairs (Table 1). Correlations with temperature (Control2/ReceiverD; r = −0.800) and stratification (Control2/ReceiverD; r = −0.722) were negative, and were stronger than other envi-

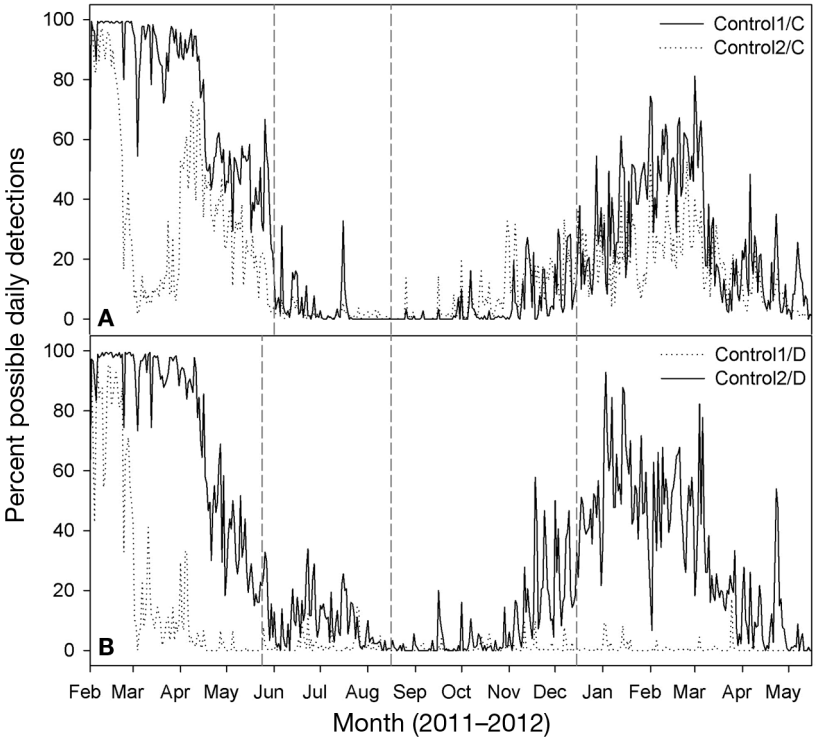

Fig. 3. Percent possible daily detections for each control tag and receiver pair. Percentages were calculated using the maximum possible detections per hour (7.5) multiplied by 24.0 h = 180.0. Tag and receiver pairs include (A) Control1/ReceiverC and Control2/ReceiverC detections and (B) Control1/ReceiverD and Control2/ReceiverD detections. Gray vertical dashed lines represent days when maintenance was performed on the array, including exchange of receivers and cleaning of tags

ronmental variables (Table 1). Correlations with swell energy (Control2/ReceiverD; r = −0.209) and along-shelf (**v**) currents (Control2/ReceiverD; r = −0.200) were also negative (Table 1). Though not correlated with all 4 tag and receiver pairs, the cross-shelf (**u**) stratification index had significant negative correlations of −0.613 and −0.621 on Control1/ReceiverC and Control2/ReceiverD, respectively (Table 1). Wave height and along-shelf (**v**) wind stress were not significantly correlated with detections for any tag and receiver pair (Table 1).

Short-term cyclic variability

Wavelet analysis revealed short-term cycles in detection data at period lengths similar to those of flood and ebb tidal current direction and speed. The global wavelet spectrum for Control1/ReceiverC was dominated by a high power around a period of 12.4 h (Fig. 4A) but was not statistically significant at any period length (Fig. 4B). When the highly variable time period from 13 April to 1 June 2011 was examined, significant peaks in power occurred at period lengths of both 6.2 and 12.4 h (Fig. 4C). The global wavelet spectrum for Control2/ReceiverC also indicated significant variability at a period length of 12.4 h and relatively strong but not statistically significant variability at about 24.0 h (Fig. 4D,E). Control1/ReceiverD had little data to be interpreted in the wavelet analysis (Fig. 4F), and no period length was found to be significant for variability during either the entire time series or more variable sections of the data (Fig. 4F,G). Strong variation was observed in Control2/ReceiverD at period lengths of 6.2, 12.4, and 24.0 h (Fig. 4H), yet none were significant for the entire dataset (Fig. 4I). When the highly variable data were examined separately, both 6.2 and 12.4 h, but not 24.0 h, were significant (Fig. 4J).

The short-term cycles detected using wavelet analysis covaried strongly with tidal current speed and direction but only weakly with the diel cycle. In general, detections were high when current speed was low around the time of slack tide and high when currents were flowing in the opposite direction of sound transmission, although there were occasions when the latter general relationship was reversed.

Table 1. Cross-correlation analysis between environmental variables and 4 tag and receiver pairs (e.g. Control1/ReceiverC denotes Control tag 1 detected on ReceiverC). Values reported are Pearson's correlation coefficients (r) for each comparison of daily detection and environmental data. **u** and **v** indicate the across- and along-shelf directions, respectively. Asterisks indicate significance using a 95% confidence interval

Variable	Control1/		Control2/	
	Rec.C	Rec.D	Rec.C	Rec.D
Temperature	−0.737*	−0.489*	−0.687*	−0.800*
Swell energy	−0.190*	−0.093*	−0.170*	−0.209*
Wave height	−0.042	0.011	0.006	−0.026
u wind stress	−0.173*	−0.062	−0.215*	−0.300*
v wind stress	−0.090	−0.005	0.041	−0.071
u current	−0.071	0.162*	0.183*	−0.092
v current	−0.187*	−0.270*	−0.290*	−0.200*
u stratification	−0.613*	−0.080	−0.272*	−0.621*
v stratification	−0.702*	−0.265*	−0.393*	−0.722*

For the comparison between Control1/ReceiverC hourly detections (Fig. 5A) and cross-shelf (**u**) currents, there was a strong peak in the periodogram at a period length of 12.8 h (Fig. 5B). A squared-coherence of 0.920 calculated at a period length of 12.8 h signifies that almost 92% of the variability in detections during the first week in May 2011 was attributable to the direction of the flood and ebb cross-shelf (**u**) tidal currents or **u** current vector (Fig. 5B). A squared-coherence of 0.750 for the comparison between detections and cross-shelf current speed (the absolute value of **u**) was also indicative of a strong relationship (Fig. 5C). The relationship between Control1/ReceiverC detections and the diel cycle was much weaker, with a squared-coherence of 0.351 (Fig. 5D). In contrast, the cross-shelf (**u**) current vector had a weak relationship (a squared coherence of 0.085) with detections on Control2/ReceiverD (Fig. 5F). Cross-shelf (**u**) current speed had the highest squared-coherence of 0.565 when compared with Control2/ReceiverD detections (Fig. 5G) and an intermediate squared coherence of 0.245 when compared with the diel cycle (Fig. 5H).

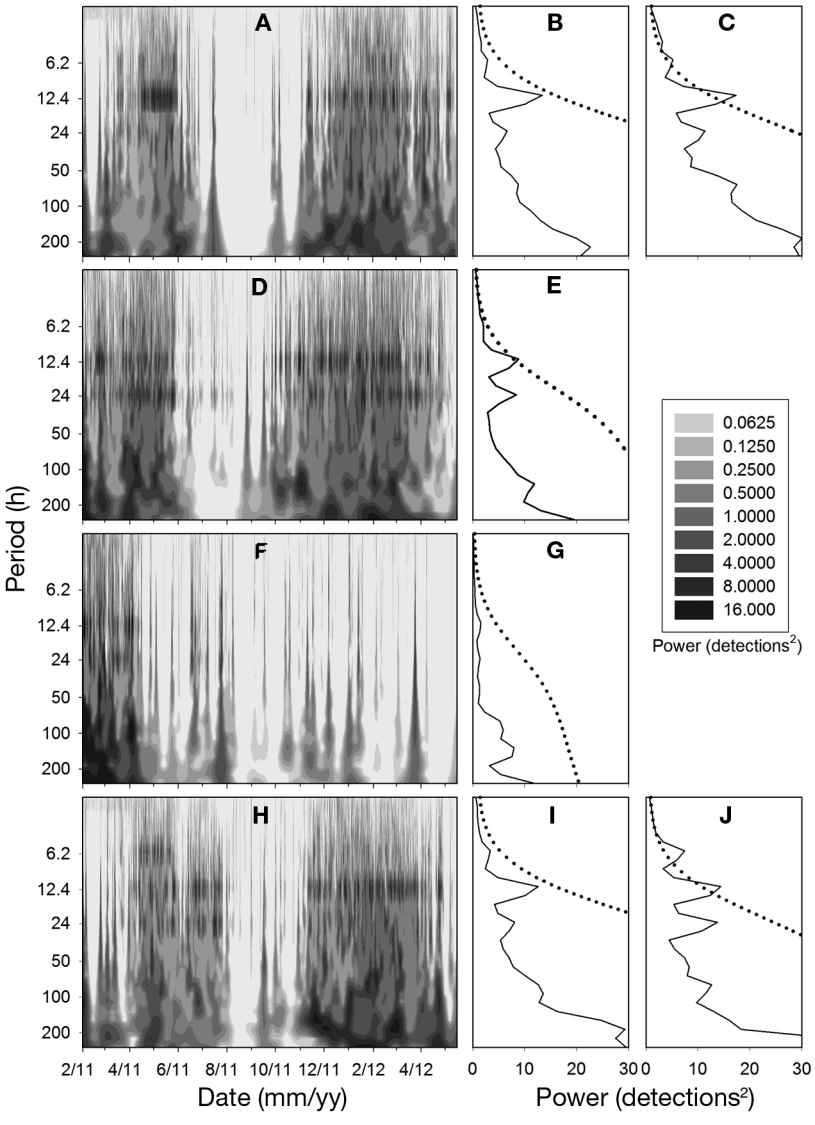

Fig. 4. Periodograms for wavelet power analysis of control tag detection data over the entire study (A,D,F, and H) and global wavelet spectra (B,C,E,G,I, and J) showing peaks at periods that dominate detection variability. Tag and receiver pairs include: (A–C) Control1/ReceiverC, (D,E) Control2/ReceiverC, (F,G) Control1/ReceiverD, and (H–J) Control2/ReceiverD. Shade intensities of wavelet power contour plots indicate the amount of variability at each period length, Power (detections)^2. The dotted line in the global wavelet spectrum graphs indicates the 95% confidence interval, such that peaks in power that cross the line are statistically significant. Control1/ReceiverC (C) and Control2/ReceiverD (J) have a second global wavelet spectrum periodogram from 13 April to 1 June 2011 and 14 April to 26 July 2011, respectively, in which a second wavelet analysis was run on only the highly variable portion of the dataset when no peaks in the periodogram were significant for the entire data record. No second global wavelet spectrum is shown for Control2/ReceiverC (D), because significant peaks were detected for the entire study period, and Control1/ReceiverD (F), because there were no significant peaks even for periods of highly variable data

Episodic variability

Synoptic-scale weather events, but not receiver maintenance, affected detections depending on the time of year and type of event. Detections decreased near the time of winter storms and increased near summer storms (Fig. 6). When detections were compared statistically before and during multiple storm events, daily detections during winter storm events were significantly lower (Wilcoxon signed rank test $p < 0.001$) compared with detections before the storms. However, daily detections during summer storms were not significantly different ($p = 0.312$) from before summer storms. There was not a significant change in detections of a tag and receiver pair following maintenance ($p = 0.074$; Fig. 3). Although episodic changes in detections were clearly related to synoptic-scale storm events,

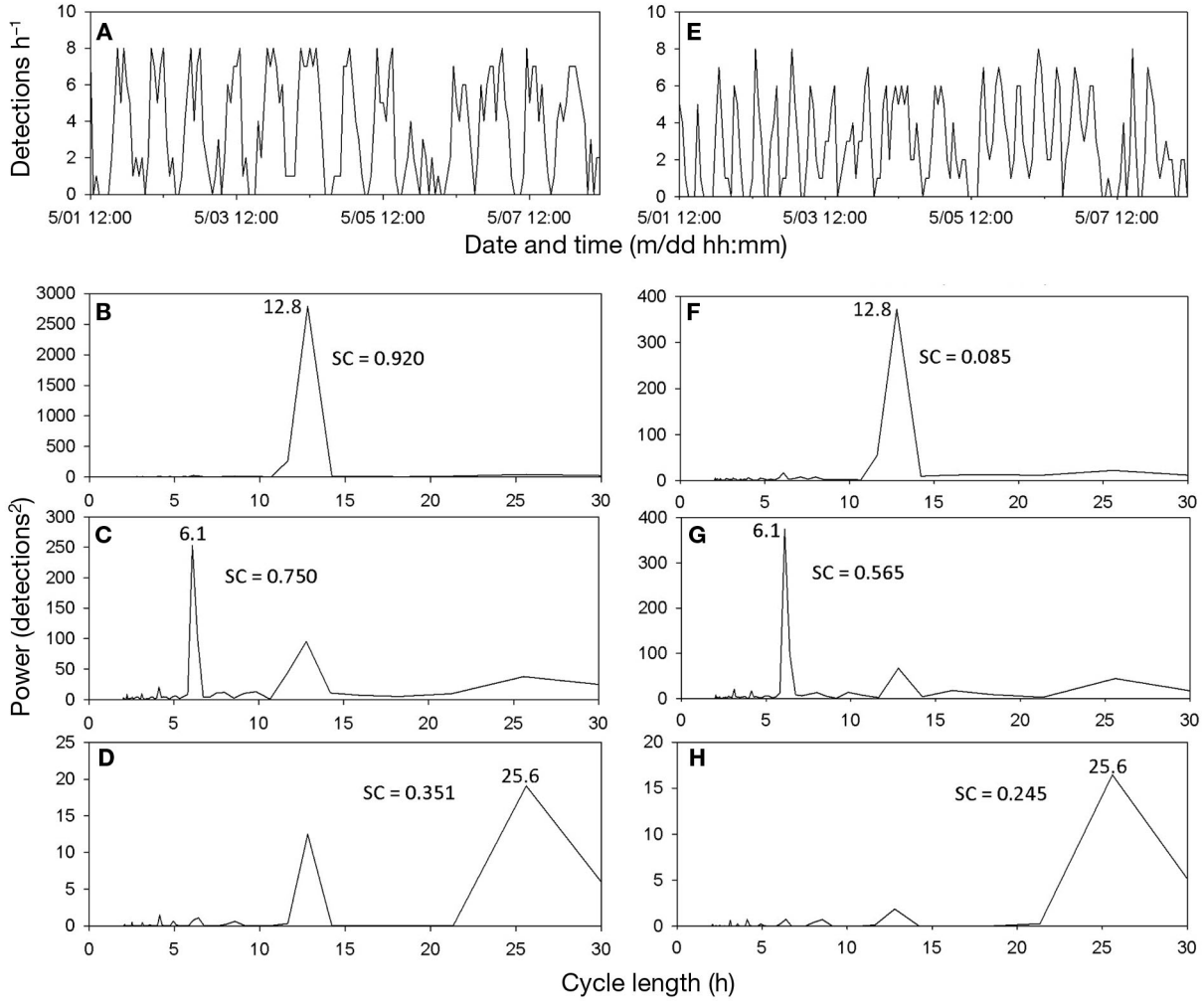

Fig. 5. Cross-Fourier analysis comparing control tag detections with environmental data during the period 1 May to 7 May 2011 for 2 control tag and receiver pairs: (A–D) Control1/ReceiverC (103 m distance) and (E–H) Control2/ReceiverD (167 m distance). Data shown include detections h^{-1} (A,E), cross-power spectral density (CPSD) comparing detections with cross-shelf (**u**) current direction (B,F), CPSD comparing detections with cross-shelf (**u**) current speed (the absolute value of **u**; C,G), and CPSD comparing detections with a diel cycle (D,H). Squared-coherence (SC) values are given for the dominant peaks in CPSD for each cross-Fourier analysis. SC can be interpreted as the proportion of variability in detections that can be explained by environmental data at the period length of maximum power

causal relationships between specific environmental variables and detections were not always obvious.

DISCUSSION

Substantial variability in the performance of the acoustic transmitter and receiver array was observed, which was related to transmission distance, seasonal and tidal cycles, and synoptic-scale weather events. Tag detections decreased with increasing distance from a receiver. This pattern was expected and has been well documented in previous studies (Topping & Szedlmayer 2011, How & de Lestang 2012, Welsh et al. 2012). It was not expected that a mean detection efficiency of <33% would be observed at a range of only 103 m. Rigorous short-term detection range tests conducted at the beginning of the Gray's Reef acoustic telemetry project in the same location and with the same acoustic equipment used in the present study had indicated a 50% detection limit of 200 m (Carroll 2010). The predicted detection range was not achieved for the duration of our study because of strong seasonal variability in detection efficiency (described below in this section). Furthermore, the range tests were conducted in March, when the results of the present study indicated detection efficiency was high, leading to an

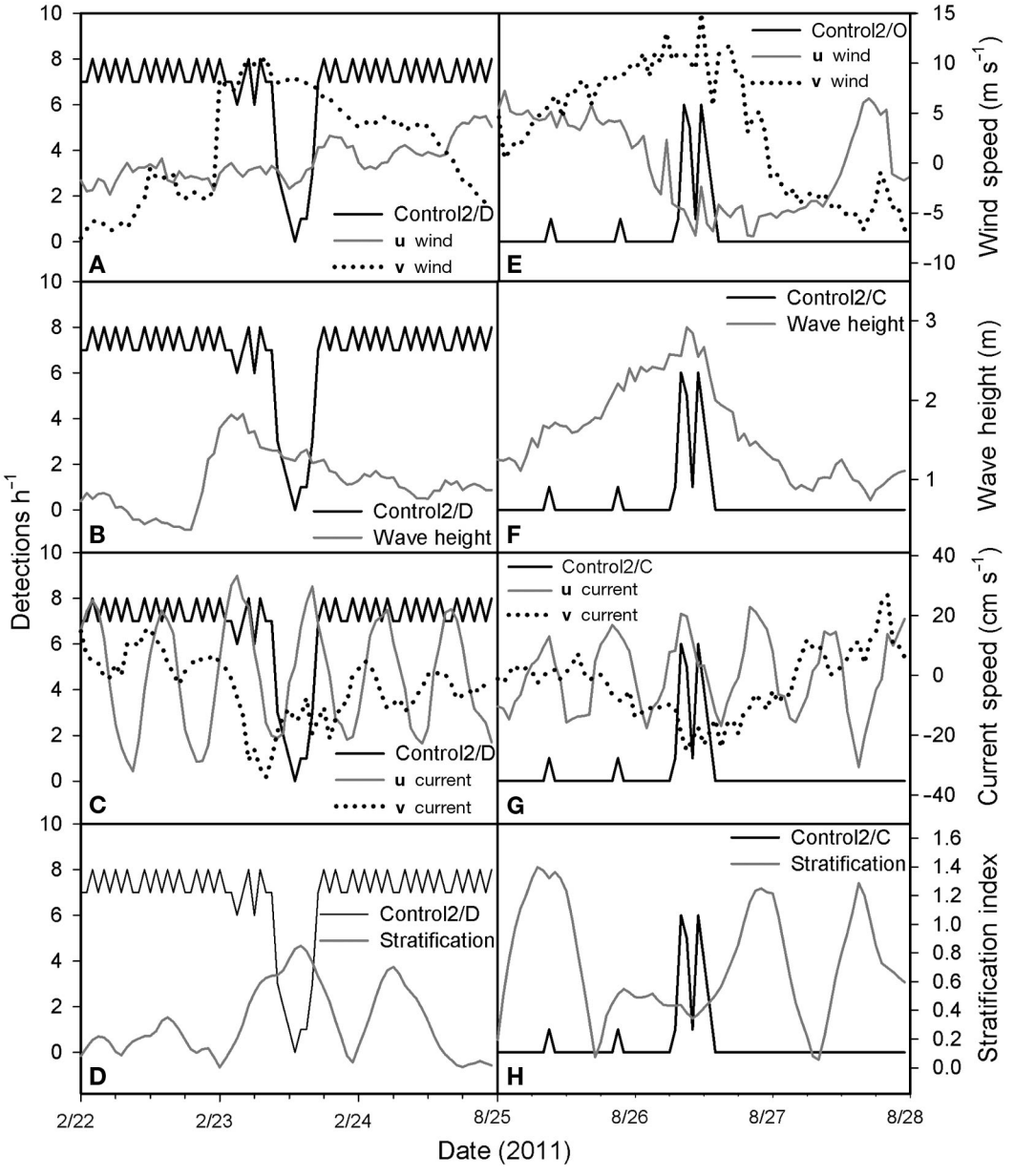

Fig. 6. Comparison of environmental data and tag detections during storm events with (A–D) Control2/ReceiverD in winter (22 February to 24 February 2011) and (E–H) Control2/ReceiverC in summer (25 August to 27 August 2011). Data shown include detections h^{-1}, cross-shelf (**u**), and along-shelf (**v**) wind stress vectors (A,E), detections h^{-1} and wave height (B,F), detections h^{-1}, cross-shelf (**u**), and along-shelf (**v**) current vectors (C,G), and detections h^{-1} and **u** stratification index (D,H)

overestimation of detection range throughout the year. This result alone highlights the importance of deploying stationary 'control' tags for the duration of acoustic telemetry studies, but detailed examination of the control tag data revealed a variety of other important considerations.

The dominant pattern in control tag detections was a seasonal pattern, with high detections in winter and low detections in summer. In winter, there were days when 100% of transmissions resulted in successful detections at a distance of 220 m, and as many as 97% of transmissions were detected at 282 m. This contrasts with summer, when there were many days when no detections were recorded on any receiver, including at 103 m, which was half the distance of the measured 50% detection range (Carroll 2010). A similar seasonal pattern was also observed in control tag detections in a study in the Gulf of Mexico, but

the mechanism behind the pattern was not explored (Topping & Szedlmayer 2011). Although there were significant correlations between detections and temperature, stratification indices, currents, swell energy, and winds in our study (Table 1), stratification (as indicated by directional differences in currents at different depths) is the most likely mechanism to result in the observed seasonal pattern in sound transmission. Changes in sound speed resulting from changes in water column properties with depth in stratified conditions cause sound waves to bend toward the bottom, resulting in a higher probability of sound attenuation or scattering due to bottom interaction compared with unstratified conditions (Kuperman & Roux 2007, Siderius et al. 2007). In a study conducted in isothermal and stratified waters 17 m deep off the coast of South Africa, Singh et al. (2009) recorded tag detections using Vemco VR2 receivers at a distance of up to 450 m when there was no stratification and only 300 m when the water column was stratified. It is important to note that a strong inverse relationship between detections and stratification was observed in our study despite the lack of detailed stratification data based on temperature, density, or salinity profiles and the use of current data for stratification indices from a buoy-mounted surface ADCP, which provides relatively poor current data compared with bottom-moored ADCPs (Seim & Edwards 2007). Alternatively, ambient noise levels could alter sound transmission (van Walree et al. 2007, Payne et al. 2010) and have been observed to be loudest in the summer and quietest in the winter (Radford et al. 2008), but no data were available to evaluate this hypothesis in our study. Regardless, it is clear that seasonal variability in sound transmission, likely due to stratification in our study, should be considered as a critical component in the design of acoustic telemetry studies.

At moderate levels of detection efficiency, near-bottom currents were the main catalyst of short-term variability in tag detections. In our study, semidiurnal tides were the primary driver of currents and resulted in strong relationships between tidal currents and detections. Cross-shelf tidal current direction at 13 m was the dominant driver of detection variability when detections were relatively high, resulting in 2 distinct peaks in detections each day (e.g. Fig. 5A) and a periodicity of 12.4 h (Fig. 5B,F). When detections were relatively low, current speed was the dominant driver of detection variability, resulting in 4 distinct peaks in detections each day during the times of tidal current minima (Fig. 5E) and a periodicity of 6.2 h (Fig. 5C,G).

The exact mechanism by which currents affected detections was not directly evaluated in our study, but potential mechanisms can be inferred from the data. First, strong currents may have tilted the receivers slightly from vertical, which might have increased detection efficiency when the receiver was tilted toward the tag. Second, even relatively slow currents can significantly alter the amplitude of sound transmission (Norton 2009). In a modeling study of the behavior of sound transmission (5 kHz) in flow, when the orientation of flow was from the receiver to the transmitter, amplitude of acoustic pulses was much greater and frequency slightly lower compared with flow from the transmitter to the receiver (Norton 2009). These first 2 mechanisms support our observation that detections were usually (although not always) higher when currents were flowing in the opposite direction of sound transmission. Third, Doppler shifts could potentially change the frequency of transmissions or alter the sensitive time intervals between individual pulses emitted by acoustic tags, which are used to determine the validity of detections and the identity of individual tags. As an acoustic transmission travels through currents flowing toward a receiver, the frequency of the pulse would increase and the time interval between pulses would decrease. Conversely, pulses traveling against the current would have a lower frequency than the original transmission and a longer interval between pulses. Such Doppler shifts of high frequency acoustic pulses have been observed in the presence of currents with slow speeds relative to the speed of sound (Preisig 2005, 2007). However, the highly detailed information on strength and timing of acoustic pulses that would be necessary to identify Doppler shifts or other effects of currents are not available from Vemco VR2W standard data downloads.

We also observed a shift in the pattern of detections as detection efficiency decreased, but did not observe the diel pattern in detections reported in other studies. As detection efficiency decreased, the pattern of detections shifted to 4 peaks each day. Detections only occurred at the slowest current speeds when conditions for sound transmission were best. Diel cycles in detections have been observed elsewhere and attributed to biological noise and wind (Payne et al. 2010, Gjelland & Hedger 2013, Koeck et al. 2013), but significant diel cycles were not detected in our study or on a shallow reef in the Great Barrier Reef, Australia (Welsh et al. 2012). Rigorous evaluation of the effects of currents and other environmental conditions (e.g. stratification, turbulence, biological noise) on acoustic receiver performance, combined with detailed data on the physical environment, is needed

to improve our understanding of the effects on acoustic signaling at frequencies used for biotelemetry. Regardless, the results of our study clearly indicate that currents, although much slower than the speed of sound, can cause significant short-term variability in the performance of acoustic arrays.

Synoptic-scale weather events (storms) resulted in episodic decreases in detection probability in most cases, but surprisingly also resulted in occasional increases in detections. It was expected that storms would cause detections to decrease due to a variety of possible factors, including noise from wind, rain, or waves, wind-driven currents, wave energy, and increased turbidity, among others. This was most obvious in winter, when detections were consistently high except for sudden, episodic declines (Fig. 6A–D). In general, sound transmission in the ocean is good in unstratified conditions, most common in winter at Gray's Reef, but storms can create conditions that increase scattering and interrupt transmission (Kuperman & Roux 2007). Although the exact mechanism interrupting sound transmission (increasing ambient noise, changing currents, increasing wave energy, increasing turbulence, increasing turbidity, etc.) could not be determined in our study from available data, there were significant decreases in detections in winter during strong northeast wind events (nor'easters). In contrast, in a few cases during late summer when detections were almost non-existent, abrupt increases in detections occurred for a short time during storms (Fig. 6E–H). This unexpected increase in detections during some storm events may have occurred due to the breakdown of stratification, which could have reduced sound attenuation due to interaction with the bottom (Kuperman & Roux 2007) or other causes. It also suggests that increasing ambient noise, wave height, and swell energy are unlikely to be the primary causes of storm-related drops in detections at Gray's Reef, as the peak in detections during some summer storms was concurrent with the peak in wind and waves (Fig. 6B). These results indicate that caution must be taken not to interpret changes in detections of tagged organisms during storms as behavior because storms can result in both increases and decreases in detections depending on environmental conditions.

Little evidence was found to support the possibility that biofouling on tags and receivers or receiver battery life reduced detections over time at Gray's Reef. No consistent spike in detections was observed when control tags were cleaned and receivers were replaced with new ones (Fig. 3). This is in contrast to Heupel et al. (2008), who found biofouling to be the main contributor to decreased detection probability with Vemco VR2 receivers in Sarasota Bay, Florida, at a depth of 3 m. However, it remains prudent to clean both stationary tags and receivers to limit any potential loss of transmission from the build-up of fouling organisms.

In summary, significant short- and long-term variability was observed in the quality of sound transmission due to environmental variability, leading to several important considerations in marine acoustic telemetry studies. (1) The detection range of acoustic arrays may vary over time at interannual, seasonal, daily, and hourly scales. The deployment of stationary control tags throughout the course of a study is necessary to understand the various environmental effects on sound transmission. (2) Relying solely on diver-performed range tests is inadequate, because diving is restricted to favorable environmental conditions, which can result in range tests that overestimate the reliable detection range. (3) Every system is different in the variety of environmental conditions that could affect sound transmission, making it critical to deploy control tags to understand local environmental effects. When the same patterns appear in animal and control tag detection data, further detailed investigation is needed to distinguish between environmental interference and animal behavior. (4) The pattern of detections from stationary control tags can vary with distance from a receiver (e.g. from constant detections to 2 or 4 peaks in detections each day in our study). Thus, it is prudent to deploy control tags at multiple distances to understand how distance affects detection efficiency. This kind of thorough investigation into environmental variability is needed for researchers to confidently ascribe patterns in acoustic detection data to animal movement.

Acknowledgements. We thank the NOAA Gray's Reef National Marine Sanctuary dive team for their tireless efforts in the field. C. Edwards and C. Natunewicz provided important comments on data analyses. Funding for our project was provided by NOAA's Living Marine Resources Cooperative Science Center grant #NA05OAR4811017 and NOAA's Gray's Reef National Marine Sanctuary.

LITERATURE CITED

Carroll CJ (2010) Using acoustic telemetry to track red snapper, gag, and scamp at Gray's Reef National Marine Sanctuary. MSc thesis, Savannah State University, Savannah, GA

DeCelles GR, Cadrin SX (2010) Movement patterns of winter flounder (*Pseudopleuronectes americanus*) in the southern Gulf of Maine: observations with the use of passive acoustic telemetry. Fish Bull 108:408–419

Edwards CR, Seim HE (2008) Complex EOF analysis as a method to separate barotropic and baroclinic velocity structure in shallow water. J Atmos Ocean Technol 25: 808–821

Gjelland KØ, Hedger RD (2013) Environmental influence on transmitter detection probability in biotelemetry: developing a general model of acoustic transmission. Methods Ecol Evol 4:665–674

Heithaus MR, Dill LM, Marshall GJ, Buhleier B (2010) Habitat use and foraging behavior of tiger sharks (*Galeocerdo cuvier*) in a seagrass ecosystem. Mar Biol 140:237–248

Heupel MR, Semmens JM, Hobday AJ (2006) Automated acoustic tracking of aquatic animals: scales, design and deployment of listening station arrays. Mar Freshw Res 57:1–13

Heupel MR, Reiss KL, Yeiser BG, Simpfendorfer CA (2008) Effects of biofouling on performance of moored data logging acoustic receivers. Limnol Oceanogr Methods 6: 327–335

How JR, de Lestang S (2012) Acoustic tracking: issues affecting design, analysis and interpretation of data from movement studies. Mar Freshw Res 63:312–324

Kendall MS, Jensen OP, Alexander C, Field D, McFall G, Bohne R, Monaco ME (2005) Benthic mapping using sonar, video transects, and an innovative approach to accuracy assessment: a characterization of bottom features in the Georgia Bight. J Coast Res 21:1154–1165

Koeck B, Alós J, Caro A, Neveu R, Crec'hriou R, Saragoni G, Lenfant P (2013) Contrasting fish behavior in artificial seascapes with implications for resources conservation. PLoS ONE 8:e69303

Kuperman W, Roux P (2007) Underwater acoustics. In: Rossing TD (ed) Springer handbook of acoustics. Springer Publishing, New York, NY, p 149–204

Large WG, Pond S (1981) Open ocean momentum flux measurements in moderate to strong winds. J Phys Oceanogr 11:324–336

Norton GV (2009) The numerical solution of acoustic propagation through dispersive moving media. In: Oceans 2009—marine technology for our future: global and local challenges. Marine Technology Society/IEEE, Biloxi, MS, p 1–6

Payne NL, Gillanders BM, Webber DM, Semmens JM (2010) Interpreting diel activity patterns from acoustic telemetry: the need for controls. Mar Ecol Prog Ser 419:295–301

Preisig JC (2005) Performance analysis of adaptive equalization for coherent acoustic communications in the time-varying ocean environment. J Acoust Soc Am 118: 263–278

Preisig JC (2007) Acoustic propagation considerations for underwater acoustic communications network development. ACM SIGMOBILE Mobile Comp Commun Rev 11: 2–10

Radford CA, Jeffs AG, Tindle CT, Montgomery JC (2008) Temporal patterns in ambient noise of biological origin from a shallow water temperate reef. Oecologia 156: 921–929

Seim HE, Edwards CR (2007) Comparison of buoy-mounted and bottom-moored ADCP performance at Gray's Reef. J Atmos Ocean Technol 24:270–284

Shanks AL (2006) Mechanisms of cross-shelf transport of crab megalopae inferred from a time series of daily abundance. Mar Biol 148:1383–1398

Siderius M, Porter MB, Hursky P, McDonald V (2007) Effects of ocean thermocline variability on noncoherent underwater acoustic communications. J Acoust Soc Am 121: 1895–1908

Simpfendorfer CA, Heupel MR, Collins AB (2008) Variation in the performance of acoustic receivers and its implication for positioning algorithms in a riverine setting. Can J Fish Aquat Sci 65:482–492

Singh L, Downey NJ, Roberts MJ, Webber DM and others (2009) Design and calibration of an acoustic telemetry system subject to upwelling events. Afr J Mar Sci 31: 355–364

Topping DT, Szedlmayer ST (2011) Site fidelity, residence time and movements of red snapper *Lutjanus campechanus* estimated with long-term acoustic monitoring. Mar Ecol Prog Ser 437:183–200

Torrence C, Compo GP (1998) A practical guide to wavelet analysis. Bull Am Meteorol Soc 79:61–78

van Walree PA, Neasham JA, Schrijver MC (2007) Coherent acoustic communication in a tidal estuary with busy shipping traffic. J Acoust Soc Am 122:3495–3506

Welsh JQ, Fox RJ, Webber DM, Bellwood DR (2012) Performance of remote acoustic receivers within a coral reef habitat: implications for array design. Coral Reefs 31: 693–702

Wing SR, Botsford LW, Largier JL, Morgan LE (1995) Spatial structure of relaxation events and crab settlement in the northern California upwelling system. Mar Ecol Prog Ser 128:199–211

Editorial responsibility: Christine Paetzold, Oldendorf/Luhe, Germany

Submitted: June 27, 2013; Accepted: October 7, 2013
Proofs received from author(s): December 12, 2013